


## Article

# Purification of High-Molecular-Weight Antibacterial Proteins of Insect Pathogenic *Brevibacillus laterosporus* Isolates

Tauseef K. Babar <sup>1,2,\*</sup> , Travis R. Glare <sup>1</sup>, John G. Hampton <sup>1</sup> , Mark R. H. Hurst <sup>3</sup>, Josefina O. Narciso <sup>1</sup> and Amy Beattie <sup>3</sup>

<sup>1</sup> Bioprotection Research Centre, Lincoln University, Lincoln 7647, Canterbury, New Zealand

<sup>2</sup> Department of Entomology, Faculty of Agricultural Sciences and Technology, Bahauddin Zakariya University, Multan 60000, Pakistan

<sup>3</sup> Resilient Agriculture, AgResearch, Lincoln Research Centre, Christchurch 8140, New Zealand

\* Correspondence: tauseefkhan@bzu.edu.pk

**Abstract:** *Brevibacillus laterosporus* (*Bl*) is a Gram-positive and spore-forming bacterium belonging to the *Brevibacillus brevis* phylogenetic cluster. Globally, insect pathogenic strains of the bacterium have been isolated, characterised, and some activities have been patented. Two isolates, *Bl* 1821L and *Bl* 1951, exhibiting pathogenicity against the diamondback moth and mosquitoes, are under development as a biopesticide in New Zealand. However, due to the suspected activity of putative antibacterial proteins (ABPs), the endemic isolates often grow erratically. Various purification methods, including size exclusion chromatography, sucrose density gradient centrifugation, polyethylene glycol precipitation, and ammonium sulphate precipitation employed in this study, enabled the isolation of two putative antibacterial proteins of ~30 and ~48 kD from *Bl* 1821L and one putative antibacterial protein of ~30 kD from *Bl* 1951. Purification of the uninduced cultures of *Bl* 1821L and *Bl* 1951 also yielded protein bands of ~30 and ~48 kD on SDS-PAGE, which indicated their spontaneous induction. A disc diffusion assay was used to determine the antagonistic activities of the putative ABPs. Subsequent transmission electron microscope (TEM) examination of a purified putative antibacterial protein-containing solution showed the presence of encapsulin (~30 kD) and polysheath (~48 kD)-like structures. Although only the ~30 kD protein was purified from *Bl* 1951, both structures were seen in this strain under TEM. Furthermore, while assessing the antibacterial activity of some fractions of *Bl* 1951 against *Bl* 1821L in the size exclusion chromatography method, the population of *Bl* 1821L persister cells was noted. Overall, this work added a wealth of knowledge about the purification of the high-molecular-weight (HMW) proteins (bacteriocins) of Gram-positive bacteria including *Bl*.

**Keywords:** antibacterial proteins; encapsulating protein; high molecular-weight bacteriocins; insect pathogenic bacterium; phage tail-like protein; purification methods



**Citation:** Babar, T.K.; Glare, T.R.; Hampton, J.G.; Hurst, M.R.H.; Narciso, J.O.; Beattie, A. Purification of High-Molecular-Weight Antibacterial Proteins of Insect Pathogenic *Brevibacillus laterosporus* Isolates. *Processes* **2022**, *10*, 1932. <https://doi.org/10.3390/pr10101932>

Academic Editor: Chi-Fai Chau

Received: 29 August 2022

Accepted: 21 September 2022

Published: 25 September 2022

**Publisher's Note:** MDPI stays neutral with regard to jurisdictional claims in published maps and institutional affiliations.



**Copyright:** © 2022 by the authors. Licensee MDPI, Basel, Switzerland. This article is an open access article distributed under the terms and conditions of the Creative Commons Attribution (CC BY) license (<https://creativecommons.org/licenses/by/4.0/>).

## 1. Introduction

Bacteriocins are ribosomally synthesised compounds released extracellularly by diverse lineages of bacteria [1,2] and are classified into two basic groups: low-molecular-weight (LMW) and high-molecular-weight (HMW) [3]. LMW bacteriocins are trypsin-sensitive, thermostable, and unsedimentable, whereas HMW bacteriocins are sedimentable, trypsin-resistant, thermolabile, and visible under an electron microscope as phage-like components [3,4]. HMW or phage tail-like bacteriocins (PTLBs), often called “tailocins” [5,6], morphologically resemble phage tails, and a common ancestral relationship between tailocins and phages has been defined [7]. Two morphologically distinct types of tailocins have been distinguished: R-type tailocins are rigid and contractile particles [8], whereas the F-type tailocins represent flexible, non-contractile structures [9]. The common feature of the two forms is how they perpetuate in nature [10]. Lysogeny is a commonly occurring

phenomenon in phages and PTLBs [11,12], and both bacterial antagonists are released upon lysis of the cell after induction [13,14]. The major components present in crude lysate apart from phages or PTLBs may include bacterial debris (mainly membranes with bacterial proteins), nucleic acids, and ribosomes [15]. To identify and characterise the protein of interest, it is vital to purify from this lysed homogenate [16,17]. A novel class of HMW complex antagonistic proteins, “encapsulins”, first identified in the supernatant of bacterium *Brevibacterium linens*, also exhibits bacteriostatic activity against various strains of *Arthrobacter*, *Bacillus*, *Brevibacterium*, *Corynebacterium*, and *Listeria* [18].

*Brevibacillus laterosporus* (*Bl*) is a Gram-positive and spore-forming bacterium belonging to the *Brevibacillus brevis* phylogenetic cluster [19]. *Brevibacillus* species are a rich source of antimicrobial peptides (AMPs) [20], and >30 AMPs, including antibacterial, antifungal, and anti-invertebrate agents, have been isolated from different species [20,21]. However, only a limited number of LMW bacteriocins have been defined [22–24]. Globally, strains of the bacterium demonstrating pathogenicity against a wide range of organisms, including insects, have been isolated, characterised [25], and some activities have been patented [26–28]. The New Zealand isolates *Bl* 1821L and *Bl* 1951 exhibit pathogenicity against the diamond-back moth, *Plutella xylostella*, and larvae of the mosquitoes (*Culex pervigilans* and *Opifex fuscus*) [27,29] and are under development as a biopesticide. However, due to the suspected activity of putative antibacterial proteins on the growth of *Bl* 1821L and *Bl* 1951, the endemic strains often lose potency [29,30]. To identify HMW antagonistic proteins (bacteriocins) belonging to different Gram-positive bacteria, various purification methods have been used [18,31–33]. However, there is limited work about the purification of HMW proteins (bacteriocins) from insect pathogenic isolates [13,34].

Herein, we describe the purification and identification of putative antibacterial proteins of *Bl* 1821L and *Bl* 1951.

## 2. Materials and Methods

### 2.1. Purification of Putative Antibacterial Proteins Using Size Exclusion Chromatography (SEC)

#### 2.1.1. Bacterial Strains and Growth Conditions

Isolates *Bl* 1821L and *Bl* 1951, held in the Bioprotection Research Centre Culture Collection, Lincoln University, New Zealand, were used in this study. Luria–Bertani medium broth (LB Miller, Sigma, St. Louis, MI, USA) was routinely used for growing bacteria on an orbital shaker (Conco, TU 4540, Taibei, Taiwan) at 250 rpm and 30 °C overnight for further usage.

#### 2.1.2. Mitomycin C Induction of Putative Antibacterial Proteins

Single colonies of bacteria were used to inoculate 5 mL of LB (Miller) broth, which was placed on an orbital shaker (Conco, TU 4540, Taibei, Taiwan) at 250 rpm and 30 °C overnight. Aliquots (500 µL) of the overnight culture were independently transferred to replicated flasks of 25 mL of LB broth. The inoculated cultures were then grown at 250 rpm and 30 °C on the orbital shaker for 10–12 h. Mitomycin C (Sigma, Sydney, NSW, Australia) was added into the flasks, which were left shaking overnight at 40 rpm and ambient temperature (24 °C). The flasks were monitored to view for signs of lysis (clearing of the culture or accumulation of bacterial debris). For *Bl* 1821L and *Bl* 1951, 1 [34] and 3 µg/mL of mitomycin C [35], respectively, was used to induce the putative antibacterial proteins with some modifications to a previously published protocol of [36].

#### 2.1.3. SEC of Putative Antibacterial Proteins

Mitomycin C-induced cultures were centrifuged at 16,000× *g* for 10 min, and the supernatants were passed through a 0.22 µm filter. Cell-free supernatants (CFS) were ultracentrifuged at 35,000 rpm (151,263× *g*) in a swing bucket rotor (41Ti, Beckman, Brea, CA, USA) for 70 min. The concentrated pellet was resuspended in 100–150 µL of TBS (Tris buffer saline: 25 mM Tris-HCl, 130 mM NaCl, pH 7.5). Prior to SEC, the resuspended pellet was passed through a 0.45 µm filter. For SEC, a Bio-Rad column (1.5 × 46 cm) was filled

with the gel matrix (Sephacryl S-400) according to the manufacturer's instructions (GE Healthcare Life Sciences, Auckland, New Zealand). Next, 800  $\mu\text{L}$  of the ultracentrifuged sample was loaded onto the SEC column (BioLogic LP System) which had been pre-equilibrated with a TBS buffer to a volume of approximately 150–200 mL at a flow rate of 1 mL/min. The sample was run at 0.5 mL/min, and the purified/separated protein mixture was monitored using a BioLogic LP System at 280 nm.

#### 2.1.4. Assay, Protein Quantification, and SDS-PAGE Analysis of SEC Fractions

Antagonistic activity of SEC-derived fractions was tested against *Bl* 1821L and *Bl* 1951 as the host bacterium through the Kirby–Bauer disc diffusion assay [37,38]. A single colony of the host bacterium was inoculated into 5 mL of LB (Miller) broth and shaken on an orbital shaker (Conco, TU-4540, Taiwan) at 250 rpm and 30 °C for 18–20 h. LB agar plates were inoculated by dipping a sterile swab into the culture and swabbed over the surface of the medium three times. The inoculum was left to dry for 10–15 min at room temperature (22 °C). A sterile 8 mm diameter paper disc (ADVANTEC, Niigata, Japan) was placed in the middle of an LB agar plate, and 80  $\mu\text{L}$  of each SEC fraction was pipetted onto the paper disc. Disc diffusion assays were performed in triplicate, assessing independently undiluted SEC fractions, from where SEC fractions exhibiting the inhibitory activities were pooled (*Bl* 1821L) and concentrated at 35,000 rpm ( $151,263\times g$ ) in a swing bucket rotor (41Ti, Beckman) for 70 min. The concentrated SEC fractions were quantified ( $\mu\text{g}/\text{mL}$ ) using a Qubit protein assay kit (Thermo Fisher Scientific, Waltham, MA, USA).

Sodium dodecyl sulphate polyacrylamide gel electrophoresis (SDS-PAGE) of SEC fractions after concentrating the putative antibacterial proteins was performed using the protocol of Laemmli [39]. Gels were run for 50 min at 200 volts and then rinsed four times with  $\text{H}_2\text{O}$  before staining with silver [40]. Five microlitres of protein ladder (BIO-RAD, Precision Plus Protein<sup>TM</sup> Standards, Auckland, New Zealand) was used.

#### 2.1.5. TEM Analysis of SEC Fractions

A 5  $\mu\text{L}$  aliquot of a SEC-purified and concentrated sample was applied to a freshly glow-discharged plastic-coated hydrophilic 200 mesh EM grid (ProSciTech; Thuringowa, Australia) and stained with 3  $\mu\text{L}$  of 0.7% uranyl acetate (UA, pH 5). The samples were examined at 18,000 to 25,000 magnification in a Morgagni 268D (FEI, Hillsboro, OR, USA) TEM operated at 80 KeV. The images were photographed using a TENGRA camera. TEM analysis was performed at AgResearch, Lincoln, New Zealand.

### 2.2. Purification of Putative Antibacterial Proteins Using Sucrose Density Gradient (SDG) Centrifugation

CFS of mitomycin C-induced cultures were ultracentrifuged as described above, and the concentrated pellet was resuspended in 100–150  $\mu\text{L}$  of a TBS buffer. Two groups of sucrose density gradients were used in this study. Group A comprising 10%, 20%, 30%, 40%, and 50% gradients and group B comprising 10%, 20%, 30%, 40%, 50%, and 60% gradients were created by applying layers of 1.25 mL of a freshly prepared sucrose solution sequentially from the greatest to the lowest sucrose concentration. After ultracentrifugation, 200  $\mu\text{L}$  of lysate (*Bl* 1821L/*Bl* 1951) was applied on top of each group of gradients and centrifuged at 35,000 rpm ( $151,263\times g$ ) in a swing bucket rotor (41Ti, Beckman) for 70 min to concentrate the putative antibacterial proteins. Similarly, CFS derived from mitomycin C-induced (without ultracentrifugation) and uninduced (without mitomycin C) cultures were independently applied (200  $\mu\text{L}$ ) at the top of both the groups of gradients to concentrate the putative antibacterial proteins. Sucrose density layers of each gradient were carefully drawn out according to the added volume and evaluated for their antagonist activities against *Bl* 1821L and *Bl* 1951 as the host bacterium using Kirby-Bauer disc diffusion assay. After assay test, volume of each gradient was made 7–7.5 mL with the TBS buffer and that pellet after resuspension in 100–150  $\mu\text{L}$  TBS buffer was further used in SDS-PAGE analysis.

Purified *Bl* 1821L putative antibacterial proteins of ~30 kD from 20% gradient (Group A) and ~48 kD from 60% gradient (Group B), and for *Bl* 1951 purified protein of ~30 kD from 50% gradient (Group A) were further concentrated and cleaned using an Amicon Ultra-0.5 (10 kD) centrifugal filter (Millipore, Cork, Ireland). SDS-PAGE analysis of mitomycin C-induced (with/without ultracentrifugation) and uninduced cultures (without mitomycin C) but with ultracentrifugation was performed as outlined above for SEC-purified fractions. Likewise, the purified and 10 kD MWCO membrane concentrated samples were also subjected to SDS-PAGE and TEM analysis.

### 2.3. Purification of Putative Antibacterial Proteins Using Polyethylene Glycol (PEG) Precipitation

Mitomycin C-induced cultures were centrifuged at  $16,000\times g$  for 10 min, and the supernatants were passed through a  $0.22\ \mu\text{m}$  filter prior to the addition of PEG 8000 (10%) and 1 M NaCl. The mixture was incubated in an ice bath for 60 min and subsequently centrifuged at  $16,000\times g$  for 30 min at  $4\ ^\circ\text{C}$ . The pellet was resuspended in 1/10th the original volume of a TBS buffer. PEG residues were removed by two sequential extractions with an equal volume of chloroform, which was combined with the resuspended pellet and vortexed for 10–15 s. The mixture was centrifuged at  $16,000\times g$  for 10 min, and the upper aqueous phase was transferred to a fresh micro centrifuge tube. This extraction process was repeated until no white interface between the aqueous and organic phases was visible. Next, PEG 8000-precipitated cultures were ultracentrifuged in a swing bucket rotor (41Ti, Beckman) at 35,000 rpm ( $151,263\times g$ ) for 70 min. The pellet was resuspended in 100–150  $\mu\text{L}$  of a TBS buffer and purified using sucrose density gradient centrifugation, concentrated by ultracentrifugation, and assessed by SDS-PAGE as outlined in the preceding section.

### 2.4. Purification of Putative Antibacterial Proteins Using Ammonium Sulphate Precipitation (ASP)

Mitomycin C-induced cultures were transferred into 50 mL tubes and centrifuged at  $10,000\times g$  for 10 min and  $4\ ^\circ\text{C}$  to remove cell debris, and the supernatants passed through a  $0.22\ \mu\text{m}$  filter. The supernatant was transferred into a 100 mL beaker with a magnetic stirrer placed in an ice bucket and precipitated using ammonium sulphate (AS) until 85% saturation was reached (calculated 85% quantity from <http://www.encorbio.com/protocols/AM-SO4.htm>, accessed on 20 November 2019). The precipitated proteins were harvested by centrifugation at  $10,000\times g$  for 20 min, and the pellets were independently resuspended in 5 mL of phosphate buffer + 150 mM NaCl. Ammonium sulphate was removed through buffer exchange using dialysis tubing and a pre-chilled phosphate buffer ( $4\ ^\circ\text{C}$ ), which was replaced every three hours. After the third buffer change, the sample within the dialysis tube was transferred into a 15 mL tube and stored at  $-80\ ^\circ\text{C}$ . Subsequently, precipitates were placed for 2–3 days in a freeze dryer maintained at  $-80\ ^\circ\text{C}$ . The precipitated cultures were dissolved in a TBS buffer and ultracentrifuged in a swing bucket rotor (41Ti, Beckman) at 35,000 rpm ( $151,263\times g$ ) for 70 min. The concentrated pellet was resuspended in 100–150  $\mu\text{L}$  of a TBS buffer. Sucrose density gradient purification was performed, and the concentrated samples were assessed by SDS-PAGE as outlined above.

## 3. Results

### 3.1. Purification of Putative Antibacterial Proteins Using SEC

#### 3.1.1. Purification of *Bl* 1821L Putative Antibacterial Protein

A disc assay test of *Bl* 1821L derived SEC fractions for activity against *Bl* 1821L and *Bl* 1951 exhibited antagonistic activity by developing a zone of inhibition with 33 of the SEC fractions against *Bl* 1821L, while 27 fractions were found active against *Bl* 1951 (Table 1; Supplementary (S) Material, Figure S1). Fractions exhibiting prominent activities were pooled (Figure S1 and Table S1), and a further assays test revealed strong differences in antagonistic activity among these pooled groups (Table S1). Pool I fractions (3, 4, 5) demonstrated antibacterial activity against both *Bl* 1821L and *Bl* 1951, but pools II (11, 12, 13, 14, 15) and III (16,17, 18, 19) had antagonistic activities only against *Bl* 1821L. Pool IV (20,

21, 22, 23, 24) displayed antibacterial activity only against *Bl* 1951, except fraction no. 21, which was active against both hosts (*Bl* 1821L and *Bl* 1951) (Table S1).

**Table 1.** *Bl* 1821L SEC active fractions of the assay test.

Host Bacterium	SEC Fractions	Total Fractions
<i>Bl</i> 1821L	2, 3, 4, 5, 6, 7, 8, 9, 10, 11, 12, 13, 14, 15, 16, 17, 18, 19, 21, 26, 27, 34, 37, 39, 40, 41, 42, 45, 49, 52, 53, 55, 58	33
<i>Bl</i> 1951	2, 3, 4, 5, 7, 8, 10, 20, 21, 22, 23, 24, 25, 26, 27, 28, 29, 30, 31, 32, 41, 42, 47, 49, 52, 59, 61	27

SDS-PAGE analysis of *Bl* 1821L various SEC fractions revealed two prominent bands of ~30 and ~48 kD molecular mass (Figure 1A). These bands were observed in pools II and III, while the ~30 kD band only was observed in pool IV. Furthermore, a faint band of ~25 kD was also visualised in pools III and IV (Figure 1A). No proteins were observed on SDS-PAGE in pool I lane (Figure 1A), although a protein was detected when measured using qubit (Table S1). Assessments of electron micrographs of SEC-purified pools revealed a hollow tube-like structure in pool III (Figure 1B) and hexagonal or phage capsid-like structures of uniform sizes in pool IV (Figure 1C).

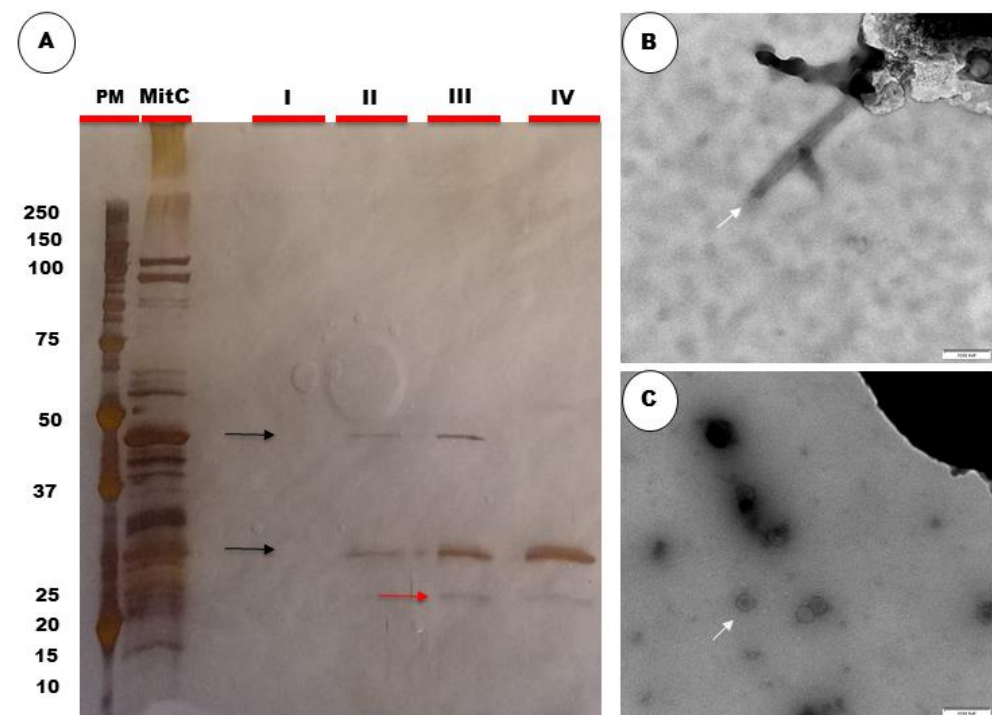


**Figure 1.** SDS-PAGE and TEM analysis of *Bl* 1821L putative antibacterial proteins purified using SEC. SDS-PAGE showing purified ~25 ((A), denoted with red arrow), ~30, and ~48 kD proteins ((A), denoted with dark arrows) of different pooled fractions. Electron micrographs of *Bl* 1821L SEC-purified putative antibacterial proteins of pool III (B) and pool IV (C). The arrows denote a hollow tube-like structure (B) and hexagonal or phage capsid-like structures of uniform size (C). Scale bar = 100 nm. PM and MitC denote protein marker and mitomycin C, respectively. MitC-induced culture cell-free supernatant was loaded into the MitC lane.

### 3.1.2. Purification of *Bl* 1951 Putative Antibacterial Protein

Of the collected 61 fractions of *Bl* 1951, fractions 6–22 (Figure S2) displayed prominent antagonistic activity in the assay tests. The quantified protein contents of SEC-purified and concentrated fractions are also presented in Table S2. Antagonistic activity of 16 SEC-derived fractions was observed against *Bl* 1951, and of 11 fractions against *Bl* 1821L as the host bacterium (Table 2). Unexpectedly, while assessing the inhibitory activity of *Bl* 1951 SEC fractions (12, 13, 14, 15, 21, 40) against *Bl* 1821L, instead of a prominent zone of inhibition, reduced growth of the host bacterium around the paper discs was observed (Figure 2), possibly indicating the presence of persister cells. These resistant cells (persister) were retrieved and cultivated overnight. Subsequent assessment of a mitomycin C-induced filtered supernatant of *Bl* 1951 against the cultivated lawn of *Bl* 1821L persister cells produced a prominent zone of inhibition (Figure 3), which suggests that the state was not maintained. As a negative control, an LB broth was used.

**Table 2.** *Bl* 1951 SEC active fractions of the assay test.

Host Bacterium	SEC Fractions	Total Fractions
<i>Bl</i> 1951	6, 9, 16, 21, 22, 27, 28, 31, 34, 40, 47, 50, 52, 55, 58, 61	16
<i>Bl</i> 1821L	8, 10, 11, 12, 13, 14, 15, 16, 18, 19, 40	11

Similar to *Bl* 1821L, some of the *Bl* 1951 SEC fractions (12, 13, 14, 15, 40) were only active against *Bl* 1821L, and some fractions (18, 21, 22, 27, 28, 61) only active against *Bl* 1951 (Figure S2 and Table 2). Assessment of these fractions by SDS-PAGE revealed the presence of a shared ~30 kD protein (Figure 4A,C). TEM examination of SEC-purified fractions no. 15 (Figure 4B) and no. 27 (Figure 4D) revealed the presence of hexagonal or phage capsid-like structures of a consistent size.

## 3.2. Purification of Putative Antibacterial Proteins Using SDG Centrifugation

### 3.2.1. Purification of *Bl* 1821L Putative Antibacterial Proteins

Antibacterial activity of *Bl* 1821L group A gradients indicated narrow zones of inhibition (9–10.5 mm) against *Bl* 1821L as the host bacterium, and assessments of group B gradients showed zones of inhibition that varied from 9 to 14 mm (Table 3). However, for *Bl* 1951 as the host bacterium, using the purified sucrose A and B gradients of both groups resulted in similar halo sizes (Table 3). SDS-PAGE analysis of *Bl* 1821L sucrose density gradients revealed the presence of two protein bands of ~30 and ~48 kD. A purified putative antibacterial protein of ~30 kD molecular mass from the 20% and 30% gradients of group A (Figure S3A) and a ~48 kD band in 20%, 40%, and 50% gradients were visualised (Figure S3A). The purified protein of ~48 kD was also prominently observed in group B gradients (40% to 60%) (Figure S3B).

SDS-PAGE analysis of uninduced (without mitomycin C) cultures of *Bl* 1821L subjected to the same purification strategy revealed the presence of a ~30 kD protein on the gel from 20% to 50% gradients of group A (Figure S4A). From these uninduced cultures, both proteins (~30 and ~48 kD) were purified and visible in group B gradients, but the ~48 kD protein was observed in gradients of 40% to 60% (Figure S4B). Mitomycin C-induced CFS of *Bl* 1821L not subjected to high-speed centrifugation was also assessed directly by SDS-PAGE with both groups of gradients, and only the ~30 kD protein was visualised in 30% and 40% gradients of group A (Figure S5).

Assessment of SDS-PAGE of group A (20%) and group B (60%) purified and 10 kD MWCO membrane concentrated solutions of *Bl* 1821L revealed prominent proteins of ~30 and ~48 kD molecular mass (Figure 5A). Electron micrographs of the concentrated solution containing a ~30 kD protein displayed globular or phage capsid-like structures (Figure 5B), and with the ~48 kD protein, long rigid polysheath-like structures were visualised (Figure 5C,D).

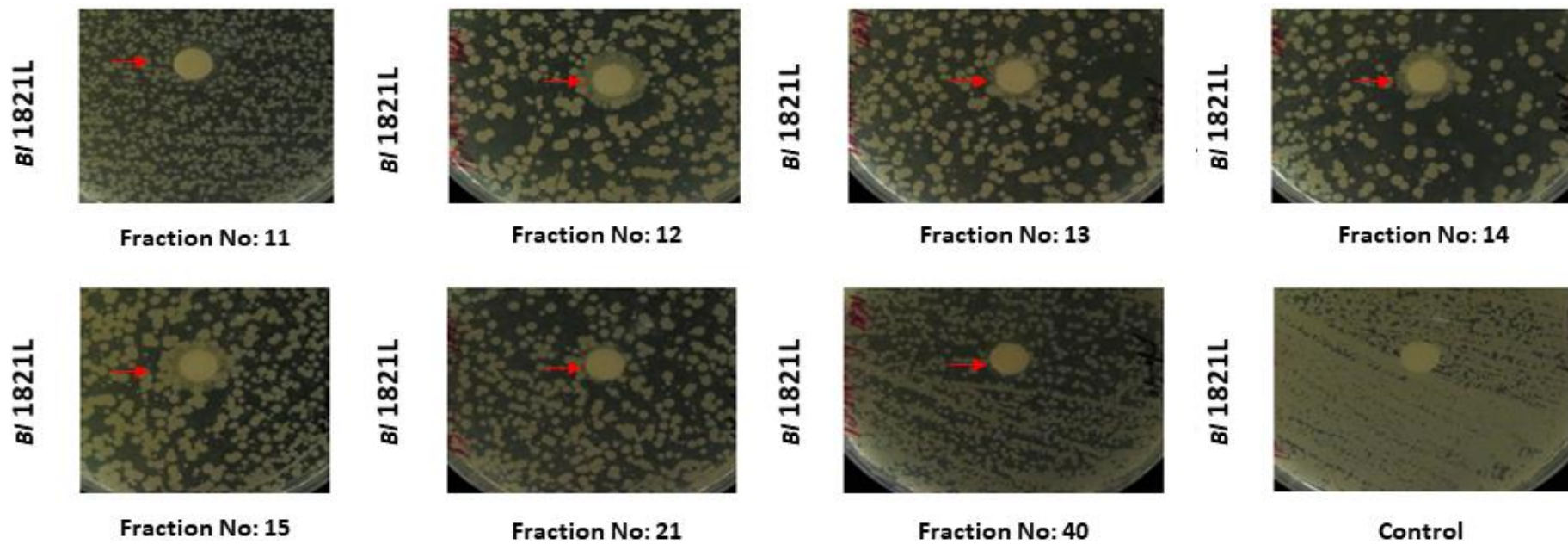
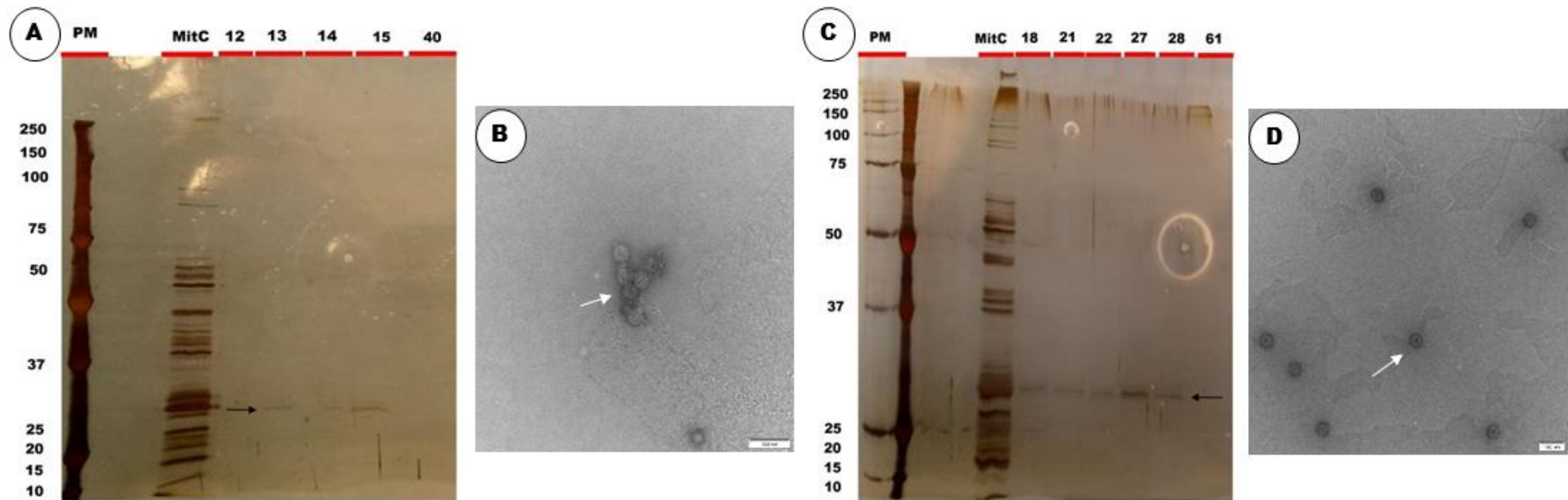


Figure 2. Disc diffusion assay test of *Bl 1951* SEC fractions against *Bl 1821L* as the host bacterium. The red arrow denotes the formed persister cells.

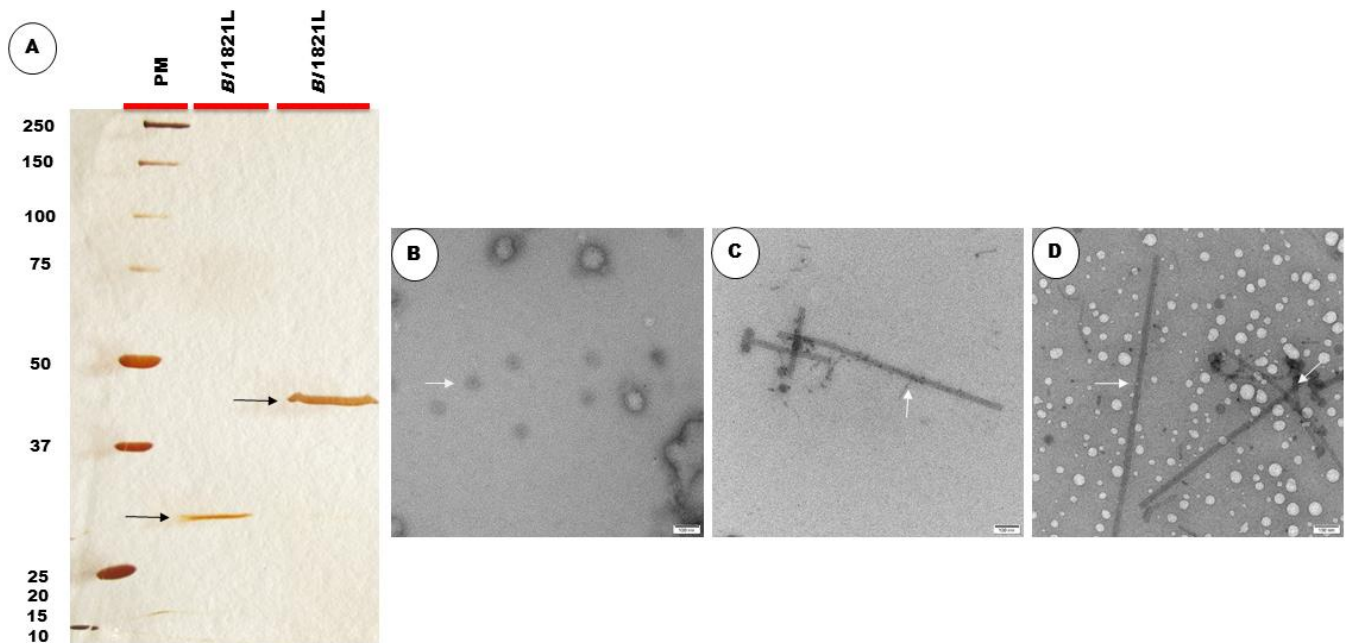


Figure 3. Disc diffusion assay test of *Bl 1951* mitomycin C-induced CFS against *Bl 1821L* persister cells. The red arrow denotes the zone of inhibition due to the activity of mitomycin C-induced CFS against the *Bl 1821L* persister cells.



**Figure 4.** SDS-PAGE and TEM analysis of *Bl* 1951 putative antibacterial protein purified using SEC. SDS-PAGES of SEC fractions 12, 13, 14, 15, 40 (A) and SEC fractions 18, 21, 22, 27, 28, 61 (C) showing a purified protein of ~30 kD (shown with a dark arrow; see SEC chromatogram, Figure S2). Electron micrographs of *Bl* 1951 SEC-purified putative antibacterial protein fraction no. 15 (B) and fraction no. 27 (D) showing uniformly sized hexagonal or phage capsid-like structures (with white arrows). Scale bar = 100 nm. PM and MitC denote protein marker and mitomycin C, respectively. MitC-induced culture cell-free supernatant was loaded into the MitC lane.





**Figure 5.** SDS-PAGE and TEM analysis of *Bl* 1821L purified and 10 kD MWCO membrane concentrated putative antibacterial proteins. SDS-PAGE analysis of *Bl* 1821L putative antibacterial proteins showing the ~30 and ~48 kD purified protein bands ((A), denoted with a dark arrow). Electron micrographs of a ~30 kD purified putative antibacterial protein showing globular or phage capsid-like structures ((B), denoted with a white arrow). TEM images of a ~48 kD purified putative antibacterial protein showing long rigid polysheath-like structures ((C,D), denoted with a white arrow). Scale bar = 100 nm. PM denotes protein marker.

**Table 3.** *Bl* 1821L putative antibacterial protein assay test and quantification using group A (10–50%) and group B (10–60%) SDGs.

Group A SDG (%)	Protein Concentration ( $\mu\text{g}/\text{mL}$ )	Zone of Inhibition Diameter (mm)		Group B SDG (%)	Protein Concentration ( $\mu\text{g}/\text{mL}$ ) (mm)	Zone of Inhibition Diameter (mm)	
		<i>Bl</i> 1821L as Host Bacterium	<i>Bl</i> 1951 as Host Bacterium			<i>Bl</i> 1821L as Host Bacterium	<i>Bl</i> 1951 as Host Bacterium
10	75.5	9.0	12.5	10	101.0	12.0	9.5
20	74.9	9.5	12.0	20	117.0	14.0	10.5
30	89.3	10.5	12.0	30	101.0	12.5	11.0
40	87.2	9.0	11.5	40	100.0	12.0	11.0
50	116.0	10.0	10.5	50	90.1	11.0	9.5
				60	84.1	9.00	9.0

### 3.2.2. Purification of *Bl* 1951 Putative Antibacterial Protein

*Bl* 1951 group A sucrose density gradients exhibited similar antagonistic activity against both hosts (*Bl* 1951 and *Bl* 1821L), producing narrow zones of inhibition (9–11.5 mm) (Table 4). Likewise, the activity of the *Bl* 1951-derived group B gradients was similar across all the gradients but slightly differed in activity from each other against the tested bacterium (Table 4). A putative antibacterial protein of ~30 kD molecular mass was purified from the crude lysate of *Bl* 1951. Excluding the uppermost gradient (10%) of both groups (A and B), the active putative antibacterial protein was purified from all the gradients (Figure S6A,B), although some other co-purified proteins were also visualised (Figure S6A).

**Table 4.** *Bl* 1951 putative antibacterial protein assay test and quantification using group A (10–50%) and group B (10–60%) SDGs.

Group A SDG (%)	Protein Concentration (µg/mL)	Zone of Inhibition Diameter (mm)		Group B SDG (%)	Protein Concentration (µg/mL)	Zone of Inhibition Diameter (mm)	
		<i>Bl</i> 1821L as Host Bacterium	<i>Bl</i> 1951 as Host Bacterium			<i>Bl</i> 1821L as Host Bacterium	<i>Bl</i> 1951 as Host Bacterium
10	88.9	9.5	9.0	10	115.0	11.5	10.0
20	84.9	9.5	9.5	20	97.5	11.5	9.0
30	77.7	9.0	9.0	30	119.0	11.0	9.0
40	75.2	9.5	10.0	40	118.0	11.0	10.0
50	92.6	9.5	11.0	50	111.0	10.5	10.5
				60	109.0	10.5	9.0

Gel electrophoresis of the *Bl* 1951 culture without mitomycin C treatment after ultracentrifugation purified a protein of ~30 kD that was visualised on SDS-PAGE across all gradients of group A and group B, except the 10% gradient (Figure S7A,B). All the gradients of group A, excluding the uppermost (10%), and group B gradients (40% to 60%) showed the ~48 kD purified protein (Figure S7B). SDS-PAGE analysis of mitomycin C-induced CFS of *Bl* 1951 without ultracentrifugation with both groups of gradients only showed the two protein bands of ~30 and ~48 kD in the top 10% and 20% gradients of group B (Figure S8).

Assessment of SDS-PAGE of group A (50%) purified and 10 kD MWCO membrane concentrated protein of *Bl* 1951 revealed a prominent protein of ~30 kD (Figure 6A). TEM examination of the concentrated *Bl* 1951 protein displayed globular or phage capsid-like structures and long nanotubes (polysheaths) (Figure 6B).

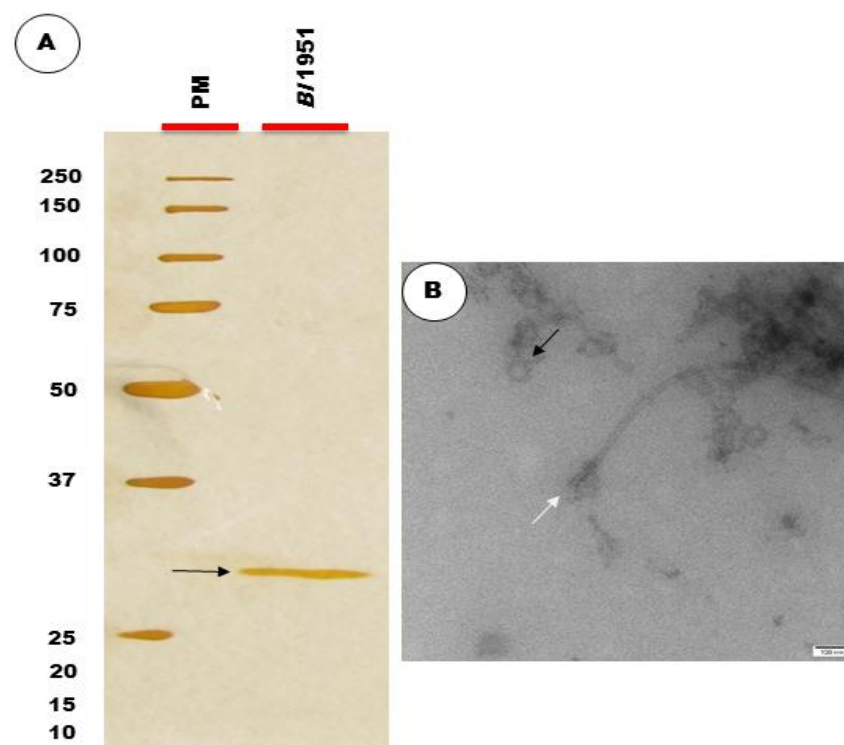


**Figure 6.** SDS-PAGE and TEM analysis of *Bl* 1951 purified and 10 kD MWCO membrane concentrated putative antibacterial protein. SDS-PAGE analysis of *Bl* 1951 putative antibacterial protein showing a ~30 kD purified protein band ((A), denoted with a dark arrow). Electron micrographs of a ~30 kD purified putative antibacterial protein of *Bl* 1951 showing globular or phage capsid-like ((B), denoted with a dark arrow) and polysheath-like structure ((B), denoted with a white arrow). Scale bar = 100 nm. PM denotes protein marker.

### 3.3. Purification of Putative Antibacterial Proteins of *Bl* 1821L Using Precipitation Methods

PEG 8000 (10%)-precipitated putative antibacterial proteins of *Bl* 1821L upon further purification with group B sucrose density gradients showed protein bands of ~30 and ~48 kD. SDS-PAGE of the PEG 8000 (10%) lysate exhibited a very minor band of ~48 kD in 40% and 60% gradients protein when compared to those of ~30 kD (Figure S9).

SDS PAGE of *Bl* 1821L ammonium-sulphate (85%)-precipitated culture with group B sucrose density gradients revealed a ~50 kD protein band from 50% and 60% gradients (Figure S10).

## 4. Discussion

Protein purification is an intrinsic step to understand the nature of a targeted protein [17]. Therefore, various methods, such as SEC, sucrose density gradient centrifugation, PEG precipitation, and ammonium sulphate precipitation were undertaken to purify the putative antibacterial proteins of insect pathogenic isolates *Bl* 1821L and *Bl* 1951. Two putative antibacterial proteins (~30 and ~48 kD) of *Bl* 1821L and one ~30 kD of *Bl* 1951 were purified. Electron micrographs of purified proteins showed different phage structural components similar to that seen in defective phages. Furthermore, SDS-PAGE of the purified products of uninduced cultures (without mitomycin C) also showed the same protein bands as mitomycin C-induced cultures. Through assessment of *Bl* 1951 SEC fractions, a population of transient resistant cells (persisters) in the *Bl* 1821L isolate was noted.

Bacteria predominantly harbour prophages in their chromosomes either in true or defective lysogenic forms [11,41] that can be induced by DNA-damaging agents such as UV radiation or mitomycin C [42,43]. The induction is suicidal for the cells as it results in bacterial cell lysis [44,45] which extracellularly releases numerous proteins apart from phages or PTLBs [15]. Therefore, to identify and characterise the protein of interest it is vital to purify from this lysed homogenate [16,17]. Ultracentrifugation is a preferred method due to its rapidity and low cost, but there are also reports that the structural components of viruses may be damaged due to the high speed [46,47]. Despite its limitations, density gradient ultracentrifugation is a common technique used to isolate and purify biomolecules and cell structures [31,46]. Purification of *Bl* 1821L putative antibacterial proteins using sucrose density gradient centrifugation showed two prominent bands of ~30 and ~48 kD molecular mass. Electron micrographs of *Bl* 1821L purified putative antibacterial proteins revealed structural differences, where phage encapsulating (capsid-like) structures were observed in a ~30 kD containing gradient. Polysheath-like structures were seen in a ~48 kD containing purified gradient, suggesting that these structures were assembled due to the polymerisation of different units. Similar polysheath structures have been defined as aberrant assemblies of tail material in a structure identical to a contracted sheath and may be found in a “smooth” or “helical” form [48]. Polysheaths are classified as phage tail-like defective bacteriophages together with rhabidosomes and particularly bacteriocins such as R-pyocins [49]. Previously, bacteria producing the long and ordered nanotube-like structures (polysheaths) were believed to harbour a true prophage, but over time, the genetic information for the phage has decreased to such an extent that the information for the sheaths is the only structural information left [48,50]. Polysheath structures are very stable and can withstand treatments with various chemical and physical factors [51,52]. Electron micrographs of the polysheath-like structures in the current study were in agreement with previous work in various bacteria [13,34,52–55]. A protein of ~30 kD molecular mass was also purified from the crude lysate of *Bl* 1951. TEM examination of the purified and 10 kD MWCO membrane concentrated solutions of *Bl* 1951 containing a ~30 kD protein revealed the presence of both globular or phage capsids-like and polysheath-like structures.

The ~30 and ~48 kD proteins were also observed in the sucrose density gradient centrifugation of non-induced (without mitomycin C) crude lysate of *Bl* 1821L and *Bl* 1951; these might be the product of spontaneous prophage induction (SPI). SPI is the activation of bacteriophages and prophage elements, pathogenicity islands, and phage morons (an extra

gene in a prophage genome without a function) from bacterial cells in the absence of an external trigger [56,57]. This phenomenon is potentially considered a detrimental process for bacterial populations, as a small percentage of cells would be lost continuously due to the lysis of the bacterial cells [56]. Earlier studies have reported the spontaneous release of free bacteriophages and phage tail-like particles in the supernatants of non-induced cultures of various lysogenic bacteria [58–60].

Size exclusion chromatography or gel filtration is a technique that is widely used to separate macromolecules based on their relative size [61,62]. Similar to sucrose density gradient centrifugation, the proteins of identical structures with equivalent molecular masses were purified. However, some differences were noted in the activity of SEC fractions. SEC pooled fractions II and III displaying both protein bands of ~30 and ~48 kD on SDS-PAGE demonstrated antagonistic activity against *Bl* 1821L, while the purified pooled IV fraction showing a ~30 kD protein was active against *Bl* 1951. Typically, the putative antibacterial proteins (bacteriocins) are antagonistic to the closely related producer bacterial strains and species, but the producer strains are immune to their lethal effects [10,14]. However, some members of a genetically identical population can kill their siblings (autocidal) [63,64]. An example is a bacteriocin hyicin 3682, which exhibits antagonistic activity against the producer strain, *Staphylococcus hyicus* [65]. The antagonistic activity of the ~30 kD encapsulating-like protein of *Bl* 1821L against *Bl* 1951 was in line with the work of various studies [18,66]. For example, Linocin M18, a putative encapsulating protein (bacteriocin) of 31 kD from *B. linens* M18 inhibits the growth of *Listeria* spp., several *Corynebacterium*, and other Gram-positive bacteria [18,66]. While purifying the putative antibacterial proteins of *Bl* 1821L using SEC, a faint band of ~25 kD was also visualised on SDS-PAGE in the pool III and pool IV fractions lane. Previously published N-terminal sequencing of a ~30 kD putative antibacterial protein of *Bl* 1821L and *Bl* 1951 identified analogous genes encoding a 25 kD hypothetical protein and a 31.4 kD putative encapsulating protein in both insect pathogenic isolates. The appearance of a 25 kD hypothetical protein might be due to co-migration [35]. Notably, some of the *Bl* 1951 SEC fractions in the assay, instead of producing a prominent zone of inhibition on the lawns of *Bl* 1821L, caused the growth of cells around the paper discs which, based on the literature, are proposed to be persister cells. All the known lineages of bacterial populations are known to harbour a small fraction of transiently antibiotic-tolerant cells known as “persisters” [67]. These cells are characterised by their dormant nature and reduced metabolic activity [68,69]. The genetic basis of persister cells formation is attributed to the role of toxin–antitoxin (TA) systems in dormancy induction [70]. Several TA systems have been suggested as the basis of persister cell formation [68,71,72]. The TA systems [73] typically consist of a stable toxin (always a protein) that disrupts an essential cellular process (e.g., translation via mRNA degradation) and a labile antitoxin (either RNA or a protein) that prevents toxicity [74]. Numerous environmental stimuli are also involved in persister cells formation [75]. It was demonstrated in [76] that DNA damage in *Escherichia coli* inducing the SOS response led to the formation of persisters by stimulating the expression of the TisB toxin. The growth phase of the bacterium plays a crucial role in determining the number of persisters, with the highest percentage of persisters found at the stationary phase [77]. Persisters are typically absent in the early exponential phase of growth, but by the mid-exponential phase, persisters begin to appear in the population, and a maximum of approximately 1% is reached during the stationary phase [77–79]. Therefore, it might be possible that in the current study, *Bl* 1821L persister cells were produced in the mid/late exponential phase, and a small percentage of these cells exhibited resistance against some of the *Bl* 1951 SEC fractions. However, *Bl* 1821L persister cells lost their resistance upon treatment with the mitomycin C-induced supernatant of *Bl* 1951, confirming their transient nature.

Protein purification through precipitation by using various salts like ammonium sulphate (AS) and polyethylene glycol (PEG) is also in use as a method to purify viral proteins (phages). PEG precipitation followed by sucrose density gradient centrifugation in SDS-PAGE analysis showed a low abundance of the ~48 kD protein band as compared

to that of ~30 kD. A putative antibacterial protein of ~50 kD was purified from the *Bl* 1821L strain after ammonium sulphate (85%) precipitation and subsequent sucrose density gradient centrifugation in the bottom 50% and 60% gradients. Since each purification step necessarily involves loss of some of the targeted proteins [80], it is possible that both precipitation methods could not purify the *Bl* 1951 putative antibacterial protein due to the involvement of several purification steps, i.e., it was lost through successive purification steps.

## 5. Conclusions

Using different classical purification methods, putative antibacterial proteins of *Bl* 1821L and *Bl* 1951 were purified and appeared as phage-like capsids (encapsulin) and polysheath-like structures under an electron microscope. Based on these observations, antibacterial activity of these preparations, and bioinformatics analyses [34,35], these antibacterial proteins are considered as HMW bacteriocins that are involved in antagonistic activities against insect pathogenic isolates *Bl* 1821L and *Bl* 1951. Although transient in nature, the appearance of persisters cells in the population of the *Bl* 1821L strain can be useful in the future to counter the lethal effects of bacterial antagonists. Overall, this work added a wealth of knowledge for the purification of HMW proteins (bacteriocins) of Gram-positive bacteria, including *Bl*.

**Supplementary Materials:** The following supporting information can be downloaded at: <https://www.mdpi.com/article/10.3390/pr10101932/s1>, Figure S1: Size exclusion chromatograph of the ultracentrifuged supernatant of a mitomycin C-induced culture of *Bl* 1821L. SEC fractions (pooled) showing putative antibacterial activity upon assessment in the disc diffusion assay are indicated. Figure S2: Size exclusion chromatograph of the ultracentrifuged supernatant of a mitomycin C-induced culture of *Bl* 1951. SEC fractions showing putative antibacterial activity upon assessment in the disc diffusion assay are indicated. Figure S3: SDS-PAGE analysis of *Bl* 1821L putative antibacterial proteins purified using sucrose density gradient (SDG) centrifugation. (A) Group A (10–50%) and (B) group B (10–60%) gradients. Figure S4: SDS-PAGE analysis of *Bl* 1821L putative antibacterial proteins from the culture without mitomycin C treatment purified using sucrose density gradient (SDG) centrifugation. (A) Group A (10–50%) and (B) group (B) (10–60%) gradients. Figure S5: SDS-PAGE analysis of *Bl* 1821L (CFS) putative antibacterial protein purified using sucrose density gradient (SDG) centrifugation. Figure S6: SDS-PAGE analysis of *Bl* 1951 putative antibacterial proteins purified using sucrose density gradient (SDG) centrifugation. (A) Group A (10–50%) and (B) group B (10–60%) gradients. Figure S7: SDS-PAGE analysis of *Bl* 1951 putative antibacterial proteins from the culture without mitomycin C treatment purified using sucrose density gradient (SDG) centrifugation (A) Group A (10–50%) and (B) group B (10–60%) gradients. Figure S8: SDS-PAGE analysis of *Bl* 1951 (CFS) putative antibacterial protein purified using sucrose density gradient (SDG) centrifugation. The red arrow denotes a faint band of ~30 kD in SDG 40%. Figure S9: SDS-PAGE analysis of *Bl* 1821L putative antibacterial proteins purified using 10% polyethylene glycol (PEG) 8000 precipitation and sucrose density gradient (SDG) centrifugation. Figure S10: SDS-PAGE analysis of *Bl* 1821L putative antibacterial protein purified using 85% ammonium sulphate precipitation (ASP) and sucrose density gradient (SDG) centrifugation. Table S1: *Bl* 1821L putative antibacterial proteins assay test and quantification of SEC fractions. Table S2: *Bl* 1951 putative antibacterial proteins assay test and quantification of SEC fractions.

**Author Contributions:** Conceptualization, T.K.B., T.R.G., and M.R.H.H.; methodology, T.K.B., T.R.G., and M.R.H.H.; validation, T.K.B., T.R.G., M.R.H.H., J.O.N., and A.B.; formal analysis, T.K.B.; investigation, T.K.B.; resources, T.R.G., M.R.H.H., and A.B.; data curation, T.K.B.; writing—original draft preparation, T.K.B.; writing—review and editing, T.R.G., J.G.H., M.R.H.H., J.O.N., and T.K.B.; visualization, T.K.B.; supervision, T.R.G., J.G.H., M.R.H.H., and J.O.N. All authors have read and agreed to the published version of the manuscript.

**Funding:** The corresponding author pursued a PhD under the Higher Education Commission (HEC) of Pakistan project “Faculty Development Programme of Bahauddin Zakariya University, Multan, Punjab, Pakistan” at the Bioprotection Research Centre, Lincoln University, Christchurch, New Zealand.

**Data Availability Statement:** All data generated or analysed during this study are included in this published manuscript and its Supplementary Materials.

**Acknowledgments:** We thank Marina Richena of Proteins and Metabolites AgResearch, Lincoln, New Zealand for her expertise in TEM analysis, and Karl Gately, Laboratory Manager, RFH building, Lincoln University, New Zealand for providing an ultracentrifugation facility for uninterrupted scientific work. Special thanks to the Lincoln University, New Zealand for granting APC funding to publish this manuscript.

**Conflicts of Interest:** The authors declare no conflict of interest.

## References

1. Ghequire, M.G.; De Mot, R. The tailocin tale: Peeling off phage tails. *Trends Microbiol.* **2015**, *23*, 587–590. [[CrossRef](#)]
2. Riley, M.A.; Wertz, J.E. Bacteriocin diversity: Ecological and evolutionary perspectives. *Biochimie* **2002**, *84*, 357–364. [[CrossRef](#)]
3. Bradley, D.E. Ultrastructure of bacteriophage and bacteriocins. *Bacteriol. Rev.* **1967**, *31*, 230–314. [[CrossRef](#)]
4. Lotz, W.; Mayer, F. Isolation and characterisation of a bacteriophage tail-like bacteriocin from a strain of *Rhizobium*. *J. Virol.* **1972**, *9*, 160–173. [[CrossRef](#)] [[PubMed](#)]
5. Ghequire, M.G.; De Mot, R. Ribosomally encoded antibacterial proteins and peptides from *Pseudomonas*. *FEMS Microbiol. Rev.* **2014**, *38*, 523–568. [[CrossRef](#)]
6. Rybakova, D.; Radjainia, M.; Turner, A.; Sen, A.; Mitra, A.K.; Hurst, M.R. Role of antifeeding prophage (Afp) protein Afp 16 in terminating the length of the Afp tailocin and stabilising its sheath. *Mol. Microbiol.* **2013**, *89*, 702–714. [[CrossRef](#)] [[PubMed](#)]
7. Nakayama, K.; Takashima, K.; Ishihara, H.; Shinomiya, T.; Kageyama, M.; Kanaya, S.; Ohnishi, M.; Murata, T.; Mori, H.; Hayashi, T. The R-type pyocin of *Pseudomonas aeruginosa* is related to P2 phage, and the F-type is related to lambda phage. *Mol. Microbiol.* **2000**, *38*, 213–231. [[CrossRef](#)] [[PubMed](#)]
8. Ge, P.; Scholl, D.; Prokhorov, N.S.; Avaylon, J.; Shneider, M.M.; Browning, C.; Buth, S.A.; Plattner, M.; Chakraborty, U.; Ding, K. Action of a minimal contractile bactericidal nanomachine. *Nature* **2020**, *580*, 658–662. [[CrossRef](#)]
9. Saha, S.; Ojober, C.D.; Mackinnon, E.; North, O.I.; Bondy-Denomy, J.; Lam, J.S.; Ensminger, A.W.; Maxwell, K.L.; Davidson, A.R. F-type pyocins are diverse non-contractile phage tail-like weapons for killing *Pseudomonas aeruginosa*. *BioRxiv* **2021**. [BioRxiv:2021.2002.2016.431561](#). [[CrossRef](#)]
10. Michel-Briand, Y.; Baysse, C. The pyocins of *Pseudomonas aeruginosa*. *Biochimie* **2002**, *84*, 499–510. [[CrossRef](#)]
11. Howard-Varona, C.; Hargreaves, K.R.; Abedon, S.T.; Sullivan, M.B. Lysogeny in nature: Mechanisms, impact and ecology of temperate phages. *Int. Soc. Microb. Ecol. J.* **2017**, *11*, 1511–1520. [[CrossRef](#)] [[PubMed](#)]
12. Tovkach, F.I. Defective lysogeny in *Erwinia carotovora*. *Microbiology* **2002**, *71*, 306–313. [[CrossRef](#)]
13. Fernández-Fernández, A.; Osuna, A.; Vilchez, S. *Bacillus pumilus* 15.1, a strain active against *Ceratitis capitata*, contains a novel phage and a phage-related particle with bacteriocin activity. *Int. J. Mol. Sci.* **2021**, *22*, 8164. [[CrossRef](#)]
14. Scholl, D. Phage tail-like bacteriocins. *Annu. Rev. Virol.* **2017**, *4*, 453–467. [[CrossRef](#)] [[PubMed](#)]
15. Boulanger, P. Purification of bacteriophages and SDS-PAGE analysis of phage structural proteins from ghost particles. In *Methods in Molecular Biology*; Clockie, M.R.J., Kropinski, M.A., Walker, M.J., Eds.; Molecular and Applied Aspects; Humana Press (Springer): Totowa, NJ, USA, 2009; Volume 2, pp. 227–238.
16. Marichal-Gallardo, P.A.; Alvarez, M.M. State-of-the-art in downstream processing of monoclonal antibodies: Process trends in design and validation. *Biotechnol. Prog.* **2012**, *28*, 899–916. [[CrossRef](#)] [[PubMed](#)]
17. Roy, I.; Mondal, K.; Gupta, M.N. Leveraging protein purification strategies in proteomics. *J. Chromatogr. B* **2007**, *849*, 32–42. [[CrossRef](#)]
18. Valdés-Stauber, N.; Scherer, S. Isolation and characterisation of Linocin M18, a bacteriocin produced by *Brevibacterium linens*. *Appl. Environ. Microbiol.* **1994**, *60*, 3809–3814. [[CrossRef](#)]
19. Shida, O.; Takagi, H.; Kadowaki, K.; Komagata, K. Proposal for two new genera, *Brevibacillus* gen. nov. and *Aneurinibacillus* gen. nov. *Int. J. Syst. Evol. Microbiol.* **1996**, *46*, 939–946. [[CrossRef](#)] [[PubMed](#)]
20. Yang, X.; Yousef, A.E. Antimicrobial peptides produced by *Brevibacillus* spp.: Structure, classification and bioactivity: A mini review. *World J. Microbiol. Biotechnol.* **2018**, *34*, 57. [[CrossRef](#)]
21. Cochrane, S.A.; Vederas, J.C. Lipopeptides from *Bacillus* and *Paenibacillus* spp.: A gold mine of antibiotic candidates. *Med. Res. Rev.* **2016**, *36*, 4–31. [[CrossRef](#)]
22. Baindara, P.; Singh, N.; Ranjan, M.; Nallabelli, N.; Chaudhry, V.; Pathania, G.L.; Sharma, N.; Kumar, A.; Patil, P.B.; Korpole, S. Laterosporulin10: A novel defensin like Class IId bacteriocin from *Brevibacillus* sp. strain SKDU 10 with inhibitory activity against microbial pathogens. *Microbiology* **2016**, *162*, 1286–1299. [[CrossRef](#)]
23. Ghadbane, M.; Harzallah, D.; Laribi, A.I.; Jaouadi, B.; Belhadj, H. Purification and biochemical characterisation of a highly thermostable bacteriocin isolated from *Brevibacillus brevis* strain GM100. *Biosci. Biotechnol. Biochem.* **2013**, *77*, 120681. [[CrossRef](#)] [[PubMed](#)]
24. Singh, P.K.; Sharma, V.; Patil, P.B.; Korpole, S. Identification, purification and characterisation of laterosporulin, a novel bacteriocin produced by *Brevibacillus* sp. strain GI-9. *PLoS ONE* **2012**, *7*, e31498.
25. Ruiiu, L. Microbial biopesticides in agroecosystems. *Agronomy* **2018**, *8*, 235. [[CrossRef](#)]

26. Baum, J.A.; CaJacob, C.A.; Feldman, P.; Heck, G.R.; Nooren, I.M.A.; Plaetinck, G.; Maddelein, W.T.; Vaughn, T.T. Methods for genetic control of insect infestations in plants and compositions thereof. U.S. Patent 10,538,783, 2020. Washington, DC: U.S. Patent and Trade Mark Office.
27. Glare, T.R.; Hampton, J.G.; Cox, M.P.; Bienkowski, D.A. Novel strains of *Brevibacillus laterosporus* as biocontrol agents against plant pests, particularly lepidoptera and diptera. *Google Patent* **2014**. World Intellectual Property Organisation International Bureau.
28. Sampson, K.S.; Tomso, D.J.; Guo, R. Pesticidal genes from *Brevibacillus* and methods for their use. U.S. Patent 9,238,823, 2016. Washington, DC: U.S. Patent and Trademark Office.
29. Ormskirk, M.M. *Brevibacillus laterosporus* as a potential biocontrol agent of the diamondback moth and other insects. Ph.D. Thesis, Lincoln University, Canterbury, New Zealand, 2017.
30. Glare, T.R.; Durrant, A.; Berry, C.; Palma, L.; Ormskirk, M.M.; Cox, M.P. Phylogenetic determinants of toxin gene distribution in genomes of *Brevibacillus laterosporus*. *Genomics* **2020**, *112*, 1042–1053. [[CrossRef](#)] [[PubMed](#)]
31. Gebhart, D.; Williams, S.R.; Bishop-Lilly, K.A.; Govoni, G.R.; Willner, K.M.; Butani, A.; Sozhamannan, S.; Martin, D.; Fortier, L.-C.; Scholl, D. Novel high-molecular-weight, R-type bacteriocins of *Clostridium difficile*. *J. Bacteriol.* **2012**, *194*, 6240–6247. [[CrossRef](#)] [[PubMed](#)]
32. Hegarty, J.P.; Sangster, W.; Ashley, R.E.; Myers, R.; Hafenstein, S.; Stewart, D.B., Sr. Induction and Purification of *Clostridium difficile* phage tail-like particles. *Methods Mol. Biol.* **2016**, *1476*, 167–175. [[CrossRef](#)]
33. Lee, G.; Chakraborty, U.; Gebhart, D.; Govoni, G.R.; Zhou, Z.H.; Scholl, D. F-type bacteriocins of *Listeria monocytogenes*: A new class of phage tail-like structures reveals broad parallel coevolution between tailed bacteriophages and high-molecular-weight bacteriocins. *J. Bacteriol.* **2016**, *198*, 2784–2793. [[CrossRef](#)] [[PubMed](#)]
34. Babar, T.K.; Glare, T.R.; Hampton, J.G.; Hurst, M.R.H.; Narciso, J.O. Isolation, purification, and characterisation of a phage tail-like bacteriocin from the insect pathogenic bacterium *Brevibacillus laterosporus*. *Biomolecules* **2022**, *12*, 1154. [[CrossRef](#)] [[PubMed](#)]
35. Babar, T.K. Heads or tails? An insight into the nature of antibacterial structures of an entomopathogenic bacterium *Brevibacillus laterosporus*. Ph.D. Thesis, Lincoln University, Canterbury, New Zealand, 2021.
36. Rybakova, D.; Mitra, A.K.; Hurst, M.R.H. Purification and TEM of Afp and Its variants. *Bio-Protocol* **2014**, *4*, e1132. [[CrossRef](#)]
37. Kirby, W.M.; Yoshihara, G.M.; Sundsted, K.S.; Warren, J.H. Clinical usefulness of a single disc method for antibiotic sensitivity testing. *Antibiot. Annu.* **1956**, 892–897. Available online: <https://pubmed.ncbi.nlm.nih.gov/13425478/> (accessed on 28 August 2022).
38. Bauer, A. Antibiotic susceptibility testing by a standardised single disc method. *Am. J. Clin. Pathol.* **1966**, *45*, 149–158. [[CrossRef](#)]
39. Laemmli, U. SDS-PAGE Laemmli method. *Nature* **1970**, *227*, 680–685. [[CrossRef](#)]
40. Blum, H.; Beier, H.; Gross, H.J. Improved silver staining of plant proteins, RNA and DNA in polyacrylamide gels. *Electrophoresis* **1987**, *8*, 93–99. [[CrossRef](#)]
41. Bobay, L.-M.; Touchon, M.; Rocha, E.P.C. Pervasive domestication of defective prophages by bacteria. *Proc. Natl. Acad. Sci. USA* **2014**, *111*, 12127–12132. [[CrossRef](#)]
42. Seaman, E.; Tarmy, E.; Marmur, J. Inducible phages of *Bacillus subtilis*. *Biochemistry* **1964**, *3*, 607–613. [[CrossRef](#)]
43. Liao, W.; Song, S.; Sun, F.; Jia, Y.; Zeng, W.; Pang, Y. Isolation, characterisation and genome sequencing of phage MZTP02 from *Bacillus thuringiensis* MZ1. *Arch. Virol.* **2008**, *153*, 1855–1865. [[CrossRef](#)]
44. Krogh, S.; Jørgensen, S.T.; Devine, K.M. Lysis genes of the *Bacillus subtilis* defective prophage PBSX. *J. Bacteriol.* **1998**, *180*, 2110–2117. [[CrossRef](#)]
45. Patz, S.; Becker, Y.; Richert-Pöggeler, K.R.; Berger, B.; Ruppel, S.; Huson, D.H.; Becker, M. Phage tail-like particles are versatile bacterial nanomachines—A mini-review. *J. Adv. Res.* **2019**, *19*, 75–84. [[CrossRef](#)]
46. Lawrence, J.E.; Steward, G.F. Purification of viruses by centrifugation. In *Manual of Aquatic Viral Ecology*; Wilhelm, S.W., Weinbauer, M.G., Suttle, C.A., Eds.; American Society of Limnology and Oceanography, Inc.: Rockville, MD, USA, 2010; pp. 166–181.
47. Børsheim, K.Y.; Bratbak, G.; Heldal, M. Enumeration and biomass estimation of planktonic bacteria and viruses by transmission electron microscopy. *Appl. Environ. Microbiol.* **1990**, *56*, 352–356. [[CrossRef](#)]
48. Kellenberger, E.; Boy de la Tour, E. On the fine structure of normal and “polymerised” tail sheath of phage T4. *J. Ultrastruct. Res.* **1964**, *11*, 545–563. [[CrossRef](#)]
49. Lotz, W. Defective bacteriophages: The phage tail-like particles. In *Progress in Molecular and Subcellular Biology*, 1st ed.; Halin, F.E., Ed.; Springer: Berlin/Heidelberg, Germany, 1976; pp. 53–102.
50. Gumpert, J.; Taubeneck, U. Microtubules in *Proteus mirabilis* as a result of defective lysogeny. *Z. Fur Allg. Mikrobiol.* **1968**, *8*, 101–105. [[CrossRef](#)]
51. Arisaka, F.; Engel, J.; Klump, H. Contraction and dissociation of the bacteriophage T4 tail sheath induced by heat and urea. *Prog. Clin. Biol. Res.* **1981**, *64*, 365–379.
52. Kurochkina, L.P.; Semenyuk, P.I.; Sykilinda, N.N.; Miroshnikov, K.A. The unique two-component tail sheath of giant *Pseudomonas* phage PaBG. *Virology* **2018**, *515*, 46–51. [[CrossRef](#)]
53. Baechler, C.A.; Berk, R.S. Electron microscopic observations of *Pseudomonas aeruginosa*. *Z. Fur Allg. Mikrobiol.* **1974**, *14*, 267–281. [[CrossRef](#)]
54. Bradley, D.; Dewar, C.A. The structure of phage-like objects associated with non-induced bacteriocinogenic bacteria. *Microbiology* **1966**, *45*, 399–408. [[CrossRef](#)]

55. Šimoliūnas, E.; Truncaitė, L.; Rutkienė, R.; Povilonienė, S.; Goda, K.; Kaupinis, A.; Valius, M.; Meškys, R. The robust self-assembling tubular nanostructures formed by gp053 from phage vB\_EcoM\_FV3. *Viruses* **2019**, *11*, 50. [[CrossRef](#)]
56. Nanda, A.M.; Thormann, K.; Frunzke, J. Impact of spontaneous prophage induction on the fitness of bacterial populations and host-microbe interactions. *J. Bacteriol.* **2015**, *197*, 410. [[CrossRef](#)]
57. Taylor, V.L.; Fitzpatrick, A.D.; Islam, Z.; Maxwell, K.L. The diverse impacts of phage morons on bacterial fitness and virulence. *Adv. Virus Res.* **2019**, *103*, 1–31. [[CrossRef](#)]
58. Lwoff, A. Lysogeny. *Bacteriol Rev* **1953**, *17*, 269–337. [[CrossRef](#)] [[PubMed](#)]
59. Smarda, J.; Benada, O. Phage tail-like (high molecular-weight) bacteriocins of *Budvicia aquatica* and *Pragia fontium* (Enterobacteriaceae). *Appl. Environ. Microbiol.* **2005**, *71*, 8970–8973. [[CrossRef](#)] [[PubMed](#)]
60. Germida, J.J. Spontaneous induction of bacteriophage during growth of *Azospirillum brasilense* in complex media. *Can. J. Microbiol.* **1984**, *30*, 805–808. [[CrossRef](#)]
61. Fekete, S.; Beck, A.; Veuthey, J.L.; Guillaume, D. Theory and practice of size exclusion chromatography for the analysis of protein aggregates. *J. Pharm. Biomed. Anal.* **2014**, *101*, 161–173. [[CrossRef](#)]
62. Jones, S.A.; Hurst, M.R. Purification of the *Yersinia entomophaga* Yen-TC toxin complex using size exclusion chromatography. *Methods Mol. Biol.* **2016**, *1477*, 39–48. [[CrossRef](#)]
63. González-Pastor, J.E.; Hobbs, E.C.; Losick, R. Cannibalism by sporulating bacteria. *Science* **2003**, *301*, 510–513. [[CrossRef](#)]
64. Popp, P.F.; Mascher, T. Coordinated cell death in isogenic bacterial populations: Sacrificing some for the benefit of many? *J. Mol. Biol.* **2019**, *431*, 4656–4669. [[CrossRef](#)]
65. Fagundes, P.C.; Ceotto, H.; Potter, A.; de Paiva Brito, M.A.V.; Brede, D.; Nes, I.F.; de Freire Bastos, M.d.C. Hyicin 3682, a bioactive peptide produced by *Staphylococcus hyicus* 3682 with potential applications for food preservation. *Res. Microbiol.* **2011**, *162*, 1052–1059. [[CrossRef](#)]
66. Eppert, I.; Valdés-Stauber, N.; Götz, H.; Busse, M.; Scherer, S. Growth reduction of *Listeria* spp. caused by undefined industrial red smear cheese cultures and bacteriocin-producing *Brevibacterium* lines as evaluated in situ on soft cheese. *Appl. Environ. Microbiol.* **1997**, *63*, 4812–4817. [[CrossRef](#)]
67. Wilmaerts, D.; Windels, E.M.; Verstraeten, N.; Michiels, J. General mechanisms leading to persister formation and awakening. *Trends Genet.* **2019**, *35*, 401–411. [[CrossRef](#)]
68. Lewis, K. Persister cells. *Annu. Rev. Microbiol.* **2010**, *64*, 357–372. [[CrossRef](#)] [[PubMed](#)]
69. Shah, D.; Zhang, Z.; Khodursky, A.B.; Kaldalu, N.; Kurg, K.; Lewis, K. Persisters: A distinct physiological state of *Escherichia coli*. *BMC Microbiol.* **2006**, *6*, 53. [[CrossRef](#)] [[PubMed](#)]
70. Jayaraman, R. Bacterial persistence: Some new insights into an old phenomenon. *J. Biosci.* **2008**, *33*, 795–805. [[CrossRef](#)] [[PubMed](#)]
71. Hong, S.H.; Wang, X.; O'Connor, H.F.; Benedik, M.J.; Wood, T.K. Bacterial persistence increases as environmental fitness decreases. *Microb. Biotechnol.* **2012**, *5*, 509–522. [[CrossRef](#)]
72. Kim, Y.; Wood, T.K. Toxins Hha and CspD and small RNA regulator Hfq are involved in persister cell formation through MqsR in *Escherichia coli*. *Biochem. Biophys. Res. Commun.* **2010**, *391*, 209–213. [[CrossRef](#)]
73. Schuster, C.F.; Bertram, R. Toxin-antitoxin systems are ubiquitous and versatile modulators of prokaryotic cell fate. *FEMS Microbiol. Lett.* **2013**, *340*, 73–85. [[CrossRef](#)]
74. Van Melderen, L.; Saavedra De Bast, M. Bacterial Toxin-antitoxin systems: More than selfish entities? *PLoS Genet.* **2009**, *5*, e1000437. [[CrossRef](#)]
75. Michiels, J.E.; Van den Bergh, B.; Verstraeten, N.; Michiels, J. Molecular mechanisms and clinical implications of bacterial persistence. *Drug Resist. Updates* **2016**, *29*, 76–89. [[CrossRef](#)]
76. Dörr, T.; Vulić, M.; Lewis, K. Ciprofloxacin causes persister formation by inducing the TisB toxin in *Escherichia coli*. *PLoS Biol.* **2010**, *8*, e1000317. [[CrossRef](#)]
77. Keren, I.; Shah, D.; Spoering, A.; Kaldalu, N.; Lewis, K. Specialised persister cells and the mechanism of multidrug tolerance in *Escherichia coli*. *J. Bacteriol.* **2004**, *186*, 8172–8180. [[CrossRef](#)]
78. Lewis, K. Multidrug tolerance of biofilms and persister cells. *Curr. Top. Microbiol. Immunol.* **2008**, *322*, 107–131. [[CrossRef](#)] [[PubMed](#)]
79. Spoering, A.L.; Lewis, K. Biofilms and planktonic cells of *Pseudomonas aeruginosa* have similar resistance to killing by antimicrobials. *J. Bacteriol.* **2001**, *183*, 6746–6751. [[CrossRef](#)]
80. Walker, J. Proteins structure, purification, characterisation, and functional analysis. In *Principles & Techniques of Biochemistry & Molecular Biology*, 6th ed.; Wilson, K., Walker, J., Eds.; Cambridge University Press: Cambridge, UK, 2005.